

# Effect of nitrogen concentration to the structural, chemical and electrical properties of tantalum zirconium nitride films

Z.Z. Tang

*School of Materials, Arizona State University, Tempe, AZ 85286, USA*

Received 2 November 2011; received in revised form 27 November 2011; accepted 28 November 2011

Available online 6 December 2011

## Abstract

Tantalum zirconium nitride films with different nitrogen concentrations were deposited by reactive co-sputtering. Systematical material characterization was done to study the effect of nitrogen concentration to the ternary nitride films' composition, microstructure, chemical and electrical properties. XRD and TEM showed that the microstructure of the films was mainly modulated by the Ta/Zr atomic ratio and nitrogen concentration, and amorphous structure formed in the nitrogen deficient films. XPS showed the chemical state of tantalum and zirconium atoms shifted systematically from metallic to ionic bonding state with the increasing of nitrogen. The stoichiometric ternary TaZrN films showed better conductivity than the binary TaN or ZrN constituents, because each tantalum atom contribute one excess d-orbital valence electron when the zirconium atom was substituted.

© 2011 Elsevier Ltd and Techna Group S.r.l. All rights reserved.

**Keywords:** C. Electrical properties; Tantalum zirconium nitride; Microstructure; XPS

## 1. Introduction

Transition metal nitride films like CrN, TiN, and ZrN have been widely used in many industries, including decoration coating, cutting tool, wear resistance and diffusion barrier in microelectronics, attributed to many attractive physical properties such as golden color, high hardness, good thermal stability and low electrical resistivity [1–8]. Recently, ternary nitride materials, which either have one more transition metal, such as TiCrN, TiZrN, and TaZrN [9–12], or another metalloid elements, such as TiSiN and TaCN [13,14], were further explored to improve the mechanical or electric properties. For example, TiZrN films showed better mechanical properties than TiN when partial of the Ti sites were substituted by Zr [12], attributed to the grain size refining effect and high activation energy for dislocation movement.

Most of the ternary nitride films reported in literatures [7–14] are stoichiometric. However, the nitrogen content in the films could significantly affect the microstructure and related physical properties. For example, tantalum nitride could have cubic, tetragonal and hexagonal structures depending on the Ta/

N ratio. In this paper, tantalum zirconium nitride films with different Ta/Zr ratios and nitrogen concentrations were deposited by co-sputtering, and the film composition, microstructure, chemical and electrical properties were systematically studied. The results showed that with the increasing of nitrogen concentration, the tantalum and zirconium atom binding energy shifted systematically from metallic to ionic state. Stoichiometric TaZrN film microstructure followed the solid solution model with the constituents of cubic phase TaN and ZrN. The electrical property of the TaZrN films was mainly modulated by the transition metal composition.

## 2. Experiments

Ternary tantalum zirconium nitride films ( $\text{Ta}_x\text{Zr}_{1-x}\text{N}_y$ ,  $(0 \leq x, y \leq 1)$ ) were deposited by magnetron co-sputtering on thermal oxidized silicon wafer. Two high purity (>99.95%) tantalum and zirconium targets were installed in the sputtering chamber and the Ta/Zr atomic ratio in the deposited TaZrN films was modulated by different power density applied on each target. Before deposition, the chamber was pumped down to base pressure around  $1 \times 10^{-4}$  Pa. The sputtering chamber was then filled with argon at a pressure of 1 Pa, and the substrates were pre-cleaned by RF argon plasma for 5 min. Nitrogen was

E-mail addresses: [Zhizhongtang@hotmail.com](mailto:Zhizhongtang@hotmail.com), [zhizhong.tang@asu.edu](mailto:zhizhong.tang@asu.edu).

introduced into the chamber as a reactive gas during film growth. The flow rate of nitrogen and argon was tuned to control the nitrogen concentration in the films. The substrate was not intentionally heated or cooled during growth.

After the ternary  $(\text{TaZr})\text{N}_y$  ( $0 \leq y \leq 1$ ) nitride films were deposited, the composition, microstructure, chemical and electrical properties of the films were systematically studied. The composition and binding energy of each element of the films were measured by X-ray photoelectron spectroscopy (XPS). Microstructure was characterized by X-ray diffraction (XRD) and transmission electron microscopy (TEM). Electrical property was measured by standard four-point probe.

### 3. Results and discussion

#### 3.1. Structure characterization

The nitrogen concentration in the ternary  $(\text{Ta}_x\text{Zr}_{1-x})\text{N}_y$  ( $0 \leq y \leq 1$ ) films increased monotonically with the nitrogen gas partial pressure (totally Ar and  $\text{N}_2$  pressure 1 Pa), as shown in Fig. 1, until it saturated at the  $\text{N}/(\text{Ta} + \text{Zr})$  ratio equal to one. Ta/Zr atomic ratio in the ternary nitride films does not affect the nitrogen concentration significantly, within the accuracy of XPS characterization. It has been proved that the limited nitrogen incorporation could facilitate the amorphization in both binary and ternary nitride materials, like TaN, TaSiN and TaCrN [15–20]. XRD and TEM showed that when the nitrogen concentration is below 37 at.% in the  $(\text{Ta}_x\text{Zr}_{1-x})\text{N}_y$  films, amorphous structure phase could be achieved. Fig. 2 shows the plain view and selected area diffraction TEM of  $\text{Ta}_{42}\text{Zr}_{31}\text{N}_{27}$  film. The plain view showed very small atomic density difference, and neither grain boundaries nor nanocrystallines were observed. The SAD TEM only showed diffused blur ring, which further confirmed the amorphous structure. When the nitrogen concentration achieves 50 at.% (stoichiometric TaZrN), only crystalline structure phase was observed. Fig. 3 shows the XRD characterization of the typical TaZrN stoichiometric films. NaCl-type face centered cubic crystal structure with strong (1 1 1) and (2 0 0) preferred orientation was observed in the XRD spectrum, indication solid solution of

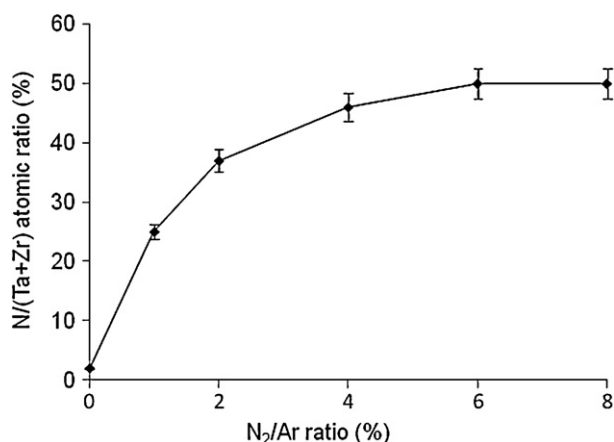


Fig. 1. The nitrogen concentration in the  $(\text{Ta}_x\text{Zr}_{1-x})\text{N}_y$  films as a function of  $\text{N}_2/\text{Ar}$  ratio.

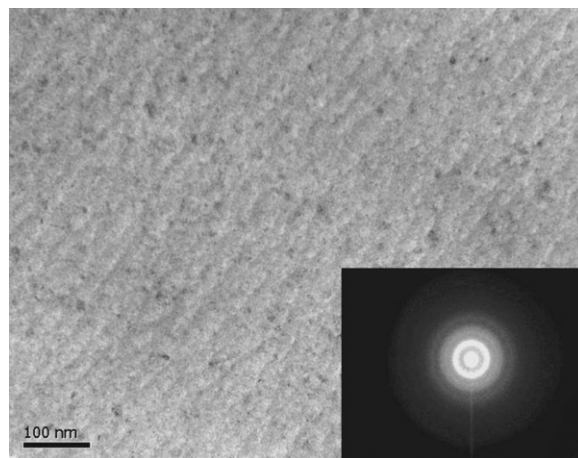


Fig. 2. Plain view and diffraction TEM observation of amorphous  $\text{Ta}_{42}\text{Zr}_{31}\text{N}_{27}$  films.

TaN and ZrN. Both TaN and ZrN have same face centered cubic (FCC) microstructure and similar lattice constant (TaN lattice constant = 4.362 Å, ZrN lattice constant = 4.577 Å) at room temperature. The lattice constant, referred based on XRD diffraction peak position, as a function of tantalum content, is shown in Fig. 4. The increase of lattice constant with increasing of Zr concentration in the TaZrN films was observed. It should be noted that in this study, no nitrogen rich ternary nitride films were observed in this study, as long as any one of the metal content (Ta or Zr) is close to 10 at.%. This is quite different to the binary metal-nitride constituents, where stable nitrogen rich phase exists, such as  $\text{Ta}_2\text{N}_3$  and  $\text{Zr}_3\text{N}_4$ . The reason why nitrogen-rich phase was not observed in this study may be related to three mechanisms. Firstly, the substrate bias and plasma enhancement et al were used to enhance the kinetic energy of nitrogen ions, thus to increase the nitrogen incorporation into nitride films, and achieve nitrogen-rich films. Without these effect during growth, the nitrogen rich phase is not preferred. Secondly, the second substitutional metal (Ta or Zr) atoms disturbed the ordering of the original binary crystal nitride structure. Thirdly, the Ta and Zr elements are not in the same group. The valence structure and grain size difference make the ordered nitrogen rich phase less possible.

#### 3.2. Chemical property

X-ray photoelectron spectroscopy (XPS) was widely used to study the organic/inorganic materials, especially thin films,

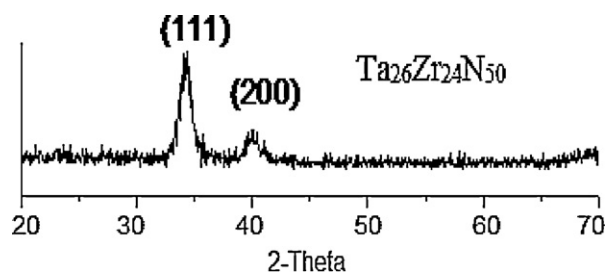


Fig. 3. XRD characterization of cubic structure  $\text{Ta}_{26}\text{Zr}_{24}\text{N}_{50}$  films with strong (1 1 1) and (2 0 0) orientation.

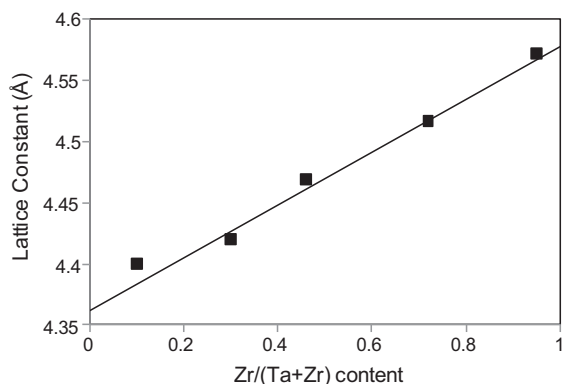


Fig. 4. Cubic structure  $(\text{Ta}_x\text{Zr}_{1-x})\text{N}$  film lattice constant with different Zr contents.

surface chemical states because of its excellent element selectivity and surface sensitivity. The significance of the tool is to reflect the bonding interaction between neighboring atoms. In this paper, XPS characterization was done to analyze the effect of nitrogen to the chemical state of transition metal elements in the  $(\text{Ta}_x\text{Zr}_{1-x})\text{N}_y$  ( $0 \leq y \leq 1$ ) films. The XPS spectra were taken in  $10^{-10}$  Torr vacuum chamber using a monochromatic Al K $\alpha$  source ( $h\nu = 1469.7$  eV) for excitation. The samples were Ar ion sputtered for around 1 min before data collection. Fig. 5(a) shows two envelope spectrum of Zr-3d, corresponding to the spin–orbit splitting of  $3d_{5/2}$  and  $3d_{3/2}$  with a band shift of about 1.5 eV, which was in a good agreement with the literature [15–17]. With the increase of nitrogen concentration, the Zr-3d peaks systematically shifted from the low binding energy (Zr- $3d_{5/2}$  178.3 eV, Zr- $3d_{3/2}$  180.8 eV, close to Zr–Zr metallic bonding state) to high binding energy (Zr- $3d_{5/2}$  179.2 eV, Zr- $3d_{3/2}$  181.7 eV, close to Zr–N ionic bonding state). With the increase of nitrogen concentration, the Ta-4d binding energy also systematically shifted from the low to high energy direction, which is shown in Fig. 5(b). The binding energy value and shift trend are consistent to the results reported in  $\text{TaN}_x$  nitride and TaZr alloy films [15]. For nitrogen N 1s, no obvious shifting was observed. As discussed in Section 3.1, nitrogen rich ternary phase was not observed in this study. This indicated that all nitrogen atoms are tightly bonded to metal atoms, for both nitrogen deficient and stoichiometric ternary films, so no clear nitrogen bonding energy shifting trend was observed.

### 3.3. Electrical properties

The electrical properties of stoichiometric  $(\text{Ta}_x\text{Zr}_{1-x})\text{N}$  films were measured by standard four-point probe. The electrical resistivity of TaZrN films with different Zr contents is shown in Fig. 6. The resistivity started from around  $400 \mu\Omega\text{-cm}$  for pure ZrN, firstly decreased to around  $150 \mu\Omega\text{-cm}$  with around 50% tantalum content, and then increased to around  $300 \mu\Omega\text{-cm}$  for pure TaN. The resistivity curve is concave shaped as a function of tantalum content. Electric conductivity is a product of carrier concentration and mobility. For ternary tantalum zirconium nitride films, the electron scattering is more significant than

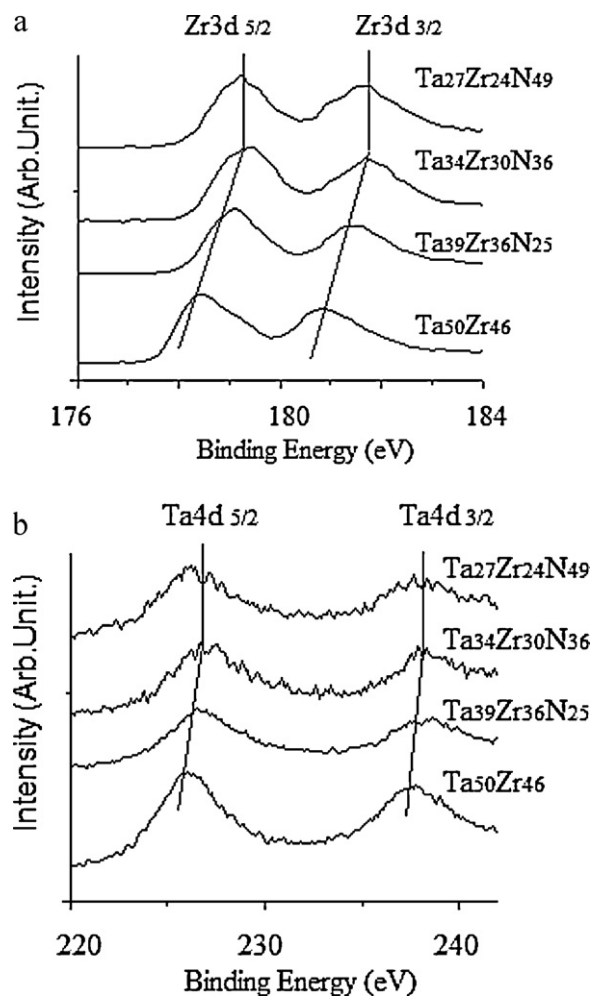


Fig. 5. XPS spectrum of tantalum zirconium nitride films, note the chemical state of Ta and Zr systematic shifting from metallic to ionic bonding state.

pure binary TaN and ZrN, so the mean free path or mobility should be shorter, if we assume similar grain boundary scattering effect. The high conductivity of ternary tantalum zirconium nitride films came from the carrier concentration increase with tantalum introduction. This can be explained by the different valence electron configuration of Zr ( $4d^25s^2$ ) and Ta ( $5d^36s^2$ ). This mechanism is very similar to the n-type

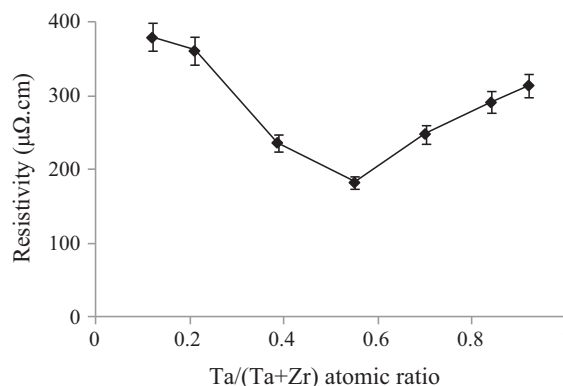


Fig. 6. Resistivity of stoichiometric TaZrN thin films with different Ta/Zr ratios.

doping in semiconductor materials. Tantalum has one more valence electron than zirconium. The TaZrN film resistivity decrease with Ta substitution of Zr has been reported [18,19]. The amorphous structure Ta–Zr alloy and other amorphous binary alloy films as Cu metallization diffusion barrier has been proposed [20–24]. It has been proved that the addition of nitrogen in to transition metal films (Ta, Zr, W, etc.) to form the crystalline or amorphous binary TaN, ZrN and WN nitride films, etc. [25–27] could further improve the barrier performance. However, the electrical properties were partially sacrificed because of the relatively high resistivity (up to 1000  $\mu\Omega\text{-cm}$ ) of the amorphous binary nitride thin films. For nitrogen deficient amorphous TaZrN films, the resistivity does not show clear relationship to composition, and the resistivity is around 400–650  $\mu\Omega\text{-cm}$  range. The high conductivity made the TaZrN ternary nitride films very promising in advanced VLSI application.

#### 4. Conclusion

Ternary tantalum zirconium nitride films were deposited by co-sputtering and the relationship of their composition, microstructure, chemical and electrical properties was systematically studied. Amorphous nitride films were observed for nitrogen deficient films. The stoichiometric TaZrN film lattice parameter follows the ideal solution model with cubic TaN and ZrN constituents. The chemical binding energy of Ta and Zr elements shifted systematically from metallic to ionic state with the increase of nitrogen concentration. The electric resistivity of TaZrN is lower than ZrN because the substitutional tantalum contributed one more d-orbital electron than zirconium.

#### References

- [1] H.O. Pierson, Handbook of Carbon, Graphite, Diamond and Fullerenes: Properties, Processing and Applications, William Andrew, 1997.
- [2] P.-L. Sun, C.-Y. Su, T.-P. Liou, C.-H. Hsu, C.-K. Lin, Mechanical behavior of TiN/CrN nano-multilayer thin film deposited by unbalanced magnetron sputter process, *J Alloys Compd.* 509 (2011) 3197–3201.
- [3] D. Liu, S.H. Yoon, B. Zhou, S.-B. Kim, H. Ahn, B.C. Prorok, S.-H. Kim, D.J. Kim, Determination of the true Young's modulus of  $\text{Pb}(\text{Zr}_{0.52}\text{Ti}_{0.48})\text{O}_3$  films by nanoindentation: effects of film orientation and substrate, *J. Am. Ceram. Soc.* 94 (2011) 3698–3701.
- [4] K. Suzuki, T. Kaneko, H. Yoshida, Y. Obi, H. Fujimori, H. Morita, Crystal structure and magnetic properties of the compound MnN, *J Alloys Compd.* 306 (2000) 66–71.
- [5] K. Radhakrishnan, N.G. Ing, R. Gopalakrishnan, Reactive sputter deposition and characterization of tantalum nitride thin films, *Mater. Sci. Eng. B* 57 (1999) 224–227.
- [6] W.-J. Chou, G.-P. Yu, J.-H. Huang, Mechanical properties of TiN thin film coatings on 304 stainless steel substrates, *Surf. Coat. Technol.* 149 (2002) 7–13.
- [7] S.H. Yoon, D. Liu, D. Shen, M. Park, D.-J. Kim, Effect of chelating agents on the preferred orientation of ZnO films by sol–gel process, *J. Mater. Sci.* 43 (2008) 6177–6181.
- [8] W. Heinke, A. Leyland, A. Matthews, G. Berg, C. Friedrich, E. Broszeit, Evaluation of PVD nitride coatings, using impact, scratch and Rockwell-C adhesion tests, *Thin Solid Films* 270 (1995) 431–438.
- [9] H. Hasegawa, A. Kimura, T. Suzuki, Microhardness and structural analysis of (Ti,Al)N, (Ti,Cr)N, (Ti,Zr)N and (Ti,V)N films, *J. Vac. Sci. Technol. A* 18 (2000) 1038–1040.
- [10] J.H. Hsieh, C. Li, C.M. Wang, Z.Z. Tang, Boundary-free multi-element barrier films by reactive co-sputtering, *Surf. Coat. Technol.* 198 (2005) 335–339.
- [11] D. Liu, B. Zhou, S.H. Yoon, Y. Wang, M. Park, B.C. Prorok, D.-J. Kim, Effects of the structural layer in MEMS substrates on mechanical and electrical properties of  $\text{Pb}(\text{Zr}_{0.52}\text{Ti}_{0.48})\text{O}_3$  films, *Ceram. Int.* 37 (2011) 2821–2828.
- [12] M.-A. Nicolet, Ternary amorphous metallic thin films as diffusion barriers for Cu metallization, *Appl. Surf. Sci.* 91 (1995) 269–276.
- [13] G. Levi, W.D. Kaplan, M. Bamberger, Structure refinement of titanium carbonitride (TiCN), *Mater. Lett.* 35 (1998) 344–350.
- [14] O. Knotek, F. Löffler, G. Krämer, Arc-deposited Ti–Zr–N coatings on cemented carbides for use in interrupted cutting, *Surf. Coat. Technol.* 49 (1991) 325–329.
- [15] R.P. Netherfield, P.J. Martin, D.R. McKenzie, Properties of  $\text{ZrN}_x$  prepared by ion-assisted deposition, *J. Mater. Sci. Lett.* 9 (1990) 972–974.
- [16] I. Bertóti, Characterization of nitride coatings by XPS, *Surf. Coat. Technol.* 152 (2002) 194–203.
- [17] Z.Z. Tang, J.H. Hsieh, S.Y. Zhang, C. Li, Phase transition and microstructure change in Ta–Zr alloy films by co-sputtering, *Surf. Coat. Technol.* 198 (2005) 110–113.
- [18] J.-L. Ruan, J.-L. Huang, H.-H. Lu, J.S. Chen, D.-F. Lii, Effects of the Ta content on the microstructure and electrical property of reactively sputtered  $\text{Ta}_x\text{Zr}_{1-x}\text{N}$  thin films, *Thin Solid Films* 519 (2011) 4987–4991.
- [19] D. Liu, W. Liu, Room temperature ultrahigh magnetoresistance nanostructure  $(\text{La}_{2/3}\text{Sr}_{1/3})\text{MnO}_3$  films growth on  $\text{SrTiO}_3$  substrate, *Ceram. Int.*, in press.
- [20] C. Li, J.H. Hsieh, Z.Z. Tang, Diffusion barriers performance of amorphous Ta–Zr films in Cu metallization, *Surf. Coat. Technol.* 202 (2008) 5676–5679.
- [21] C. Li, J.H. Hsieh, Z.Z. Tang, Study on the amorphous Ta–Zr films as diffusion barrier in Cu metallization, *J. Vac. Sci. Technol. A* 26 (2008) 980–984.
- [22] D. Liu, W. Liu, Growth and characterization of epitaxial  $(\text{La}_{2/3}\text{Sr}_{1/3})\text{MnO}_3$  films by pulsed laser deposition, *Ceram. Int.* 37 (2011) 3531–3534.
- [23] C. Li, J.H. Hsieh, Z.Z. Tang, J.-C. Cheng, Parametric and numerical study on the diffusion in a metalized amorphous binary alloys film, *Thin Solid Films* 517 (2009) 5087–5091.
- [24] C. Li, J.H. Hsieh, Z.Z. Tang, J.-C. Cheng, A diffusion study in the barrier of metallized amorphous binary alloys with numerical approach, *Thin Solid Films* 517 (2009) 3831–3836.
- [25] J.-L. Ruan, D.-F. Lii, J.S. Chen, J.-L. Huang, Investigation of substrate bias effects on the reactively sputtered ZrN diffusion barrier films, *Ceram. Int.* 35 (2009) 1999–2005.
- [26] G.S. Chen, S.T. Chen, Diffusion barrier properties of single- and multi-layered quasi-amorphous tantalum nitride thin films against copper penetration, *J. Appl. Phys.* 87 (2000) 8473–8482.
- [27] B.-S. Suh, Y.-J. Lee, J.-S. Hwang, C.-O. Park, Properties of reactively sputtered  $\text{WN}_x$  as Cu diffusion barrier, *Thin Solid Films* 348 (1999) 299–303.